arXiv:1402.1351v1 [cond-mat.mes-hall] 6 Feb 2014

Pump-probe scheme for electron-photon dynamics in hybrid conductor-cavity systems

T. L. van den Berg, C. Bergenfeldt, and P. Samuelsson
Physics department, Lund University, Box 118, S-221 00 Lund, Sweden
(Dated: February 7, 2014)

Recent experiments on nanoscale conductors coupled to microwave cavities put in prospect transport investigations of electron-photon interplay in the deep quantum regime. Here we propose a pump-probe scheme to investigate the transient dynamics of individual electron-photon excitations in a double quantum dot-cavity system. Excitations pumped into the system decay via charge tunneling at the double dot, probed in real time. We investigate theoretically the short-time charge transfer statistics at the dot, for periodic pumping, and show that this gives access to vacuum Rabi oscillations as well as excitation dynamics in the presence of double dot dephasing and relaxation.

PACS numbers: 73.23.Hk, 72.10.Di, 85.25.-j

Introduction.– Hybrid quantum electrodynamic (QED) structures that incorporate nanoscopic conductors in superconducting circuits have attracted a lot of interest over the last few years. Several experiments have demonstrated coupling between both single [1–3] and double [4–9] quantum dots (DQDs) and a superconducting microwave cavity. Hybrid conductor-cavity systems have large potential for applications in quantum information technology [10–12] and can be used as a characterization tool for nanoscale systems [13–15]. Moreover, they put in prospect transport investigations as well as applications of electron-photon interactions in the deep quantum limit [16–20]. This includes DQD masers [21, 22, 22], entanglement detection in Cooper-pair splitters [23], testbeds for Franck-Condon physics [24], detection schemes for Majorana fermions [25–27], photon emission statistics [28] and efficient heat engines [29].

A key feature of nanoscopic conductor-cavity system which to date has received little attention is the dynamics of electron-photon excitations. Besides being of fundamental interest and of importance for conductor-cavity applications, knowledge of the dynamics is instrumental in identifying and characterizing parasitic effects responsible for excitation dephasing and relaxation [30]. However, an experiment investigating the dynamics would arguably require, in the same conductor-cavity system, both short time excitation manipulation and detection. Importantly, in circuit QED systems microwave photons can be generated and controlled in real time with large accuracy [31–33]. Moreover, time resolved counting of electrons in quantum dot systems has been demonstrated experimentally [34, 35].

In this letter we combine these two capacities and propose a *pump-probe* scheme for investigating the transient dynamics of electron-photon excitations in a hybrid conductor-cavity system (See Fig. 1). Single excitations are pumped into the system via an externally driven qubit coupled to the cavity. The excitations relax by electron tunneling at the DQD, probed by monitoring the dot occupation in real time. We analyze theoretically the short time charge transport statistics at the DQD for periodic pumping, and show that it provides information on vacuum Rabi oscillations, as well as excitation relaxation time scales. Moreover, the transport statistics clearly displays how DQD dephasing and relaxation alter the dynamics, key knowledge in the experimental efforts to reach the strong conductor-cavity coupling regime.

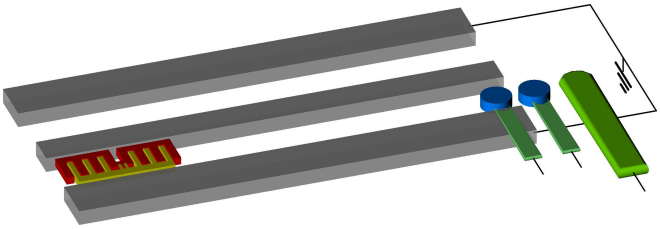

FIG. 1: (color online) Schematic of the hybrid system. An externally excited qubit (left) and a double quantum dot (right) are coupled to a coplanar superconducting microwave cavity. Further, one of the quantum dots is coupled to a lead.

System.– The system under investigation consists of a DQD coupled to a superconducting microwave cavity, and tunnel coupled to a single lead electrode. The DQD, occupied with at most one excess electron, contains two active levels. Moreover, an externally controlled superconducting qubit, in Fig. 1 exemplified by a transmon [36], is coupled to the cavity. The DQD and the qubit are coupled to the cavity with the same strength g_0, and kept at resonance with the fundamental cavity mode, at frequency ω_0. In addition the characteristic impedance Z_0 of the cavity is taken much smaller than the resistance quantum $R_Q = h/e^2$. Under these conditions the DQD-cavity-qubit system is described by the generalized Tavis-Cummings (TC) Hamiltonian

$$\hat{H}_S = \hbar\omega_0 \hat{a}^\dagger \hat{a} + \frac{\hbar\omega_0}{2}\left(\hat{\sigma}_z + \hat{d}_e^\dagger \hat{d}_e - \hat{d}_g^\dagger \hat{d}_g\right) + \hbar g_0 \left[\hat{a}^\dagger(\hat{\sigma}_- + \hat{d}_g^\dagger \hat{d}_e) + \hat{a}(\hat{\sigma}_+ + \hat{d}_e^\dagger \hat{d}_g)\right]. \quad (1)$$

Here $\hat{a}^\dagger$ (a) is the photon creation (annihilation) operator, and $\hat{d}_{e/g}^\dagger$ ($\hat{d}_{e/g}$) the electron creation (annihilation) operators for the excited/ground (bonding/anti-bonding)

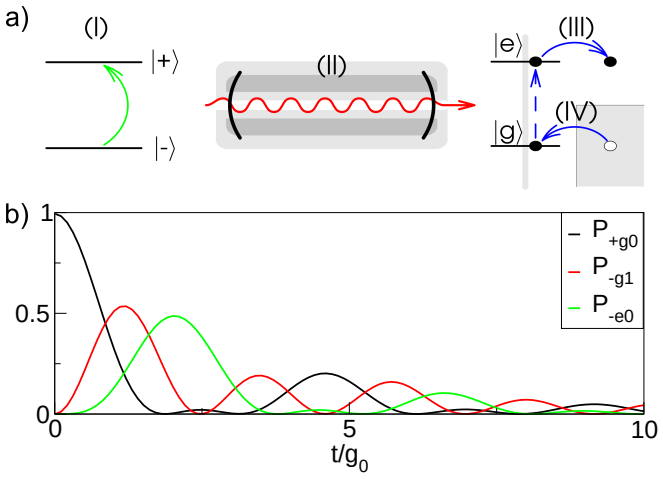

FIG. 2: (color online) a) Complete excitation transfer cycle: (I) The qubit is excited by a fast pulse. (II) The qubit decays by emitting a photon into the cavity. (III) The dot electron absorbs the cavity photon and tunnels out to the lead. (IV) A lead electron tunnels into the ground state of the dot, leaving an electron-hole pair excitation in the lead. b) Decay of vacuum Rabi oscillations for $\Gamma = g_0$. Probabilities as a function of time for the states $|+g0\rangle, |-g1\rangle, |-e0\rangle$ shown.

states of the DQD. The qubit operators $\hat{\sigma}_\pm = \hat{\sigma}_x \pm \mathrm{i}\hat{\sigma}_y$ and $\hat{\sigma}_z$ are expressed in Pauli matrices. In the local basis $|\pm\rangle$ denote the excited/ground state of the qubit, $|e/g/0\rangle$ describe the DQD in the excited/ground state or unoccupied and $|p\rangle$ the cavity state with p photons. Throughout the paper we neglect qubit decoherence and cavity losses, a reasonable assumption based on circuit QED experiments, see e.g. [37–39]. A discussion of DQD dephasing and relaxation is deferred to the last paragraph.

Single excitation dynamics – To provide a basic picture of the dynamics we first consider a single excitation of the isolated DQD-cavity-qubit system. By applying an appropriate sequence of fast pulses, on a nanosecond time scale, the qubit is excited, see e.g. [32, 40]. This can be described by the operator $\hat{R} = (\hat{\sigma}_+ + \hat{\sigma}_-)/2 = \hat{\sigma}_x$. Starting in the system ground state, exciting the qubit gives $|-g0\rangle \rightarrow |+g0\rangle$. Since $|+g0\rangle$ is no eigenstate of the TC-Hamiltonian, following the excitation at $t = 0$ the system undergoes a free, coherent time evolution described by the wavefunction

$$|\Psi(t)\rangle = (1/\sqrt{2})\left[\cos^2\left(g_0 t/\sqrt{2}\right)|+g0\rangle + \sin^2\left(g_0 t/\sqrt{2}\right)|-e0\rangle + (i/\sqrt{2})\sin\left(\sqrt{2}g_0 t\right)|-g1\rangle\right]. \quad (2)$$

This shows that the system performs vacuum Rabi oscillations, i.e. the excitation oscillates between the qubit and the DQD, via the cavity, with a frequency $\sqrt{2}g_0$.

Turning to the transport setup in Fig. 1, with the DQD coupled to a lead electrode, the result in Eq. (2) is modified. The lead, at thermal equilibrium with a temperature T and chemical potential μ, is described with the Hamiltonian $\hat{H}_L = \sum_k \epsilon_k \hat{c}_k^\dagger \hat{c}_k$, where $\hat{c}_k^\dagger$ denotes the creation operator for an electron at energy ϵ_k. We will take the detuning between levels in the dots, forming the DQD, to be zero. For this case the effective lead-DQD tunneling amplitudes are equal for $|e\rangle$ and $|g\rangle$. The tunnel Hamiltonian is then given by $\hat{H}_T = \sum_{k,\alpha=e,g} t_k \hat{c}_k^\dagger \hat{d}_\alpha + H.c.$.

We consider the sequential tunneling regime $\Gamma \ll \hbar\omega$, with $\Gamma = 2\pi \sum_k |t_k|^2 \delta(\epsilon_k \pm \hbar\omega_0/2)$ the DQD-tunneling rate. Applying the Born-Markov approximation a quantum master equation (QME) $d\hat{\rho}/dt = \mathcal{L}\hat{\rho}$ is derived for the time evolution of the reduced qubit-DQD-cavity system density operator $\hat{\rho}$. By taking $\mu = 0$ and $\hbar\omega_0/2 \gg k_B T$ the occupation of the lead at the energies at which electrons tunnel into or out of the DQD does not depend on the temperature. The Liouvillian $\mathcal{L}$ then becomes

$$\mathcal{L}\hat{\rho} = -\frac{i}{\hbar}[\hat{H}_S, \hat{\rho}] + \frac{\Gamma}{2}\left[\mathcal{D}(\hat{\rho}, \hat{d}_e^\dagger) + \mathcal{D}(\hat{\rho}, \hat{d}_g)\right], \quad (3)$$

with $\mathcal{D}(\hat{\rho}, \hat{\gamma}) = 2\hat{\gamma}^\dagger\hat{\rho}\hat{\gamma} - \hat{\gamma}\hat{\gamma}^\dagger\hat{\rho} - \hat{\rho}\hat{\gamma}\hat{\gamma}^\dagger$ for any operator $\hat{\gamma}$.

The system dynamics after an excitation at $t = 0$ is illustrated in Fig. 2. The vacuum Rabi oscillations decay, with the excited state probabilities $\propto e^{-\Gamma t/4}$ for $\Gamma \ll g_0$. Hence, the system excitation is eventually transformed into an electron-hole pair excitation in the lead as $|-e0\rangle \rightarrow |-00\rangle \rightarrow |-g0\rangle$, i.e. the DQD electron, in $|e\rangle$, tunnels out into the lead followed by a back tunneling into $|g\rangle$.

Pump-probe scheme – We consider an experimentally relevant pump-probe scheme, with a periodic pumping, or excitation, of the qubit. Importantly, the pump period τ constitutes a versatile tool for investigating the different time scales of the dynamics. We focus on periodic steady-state operation, where the state of the system is entirely determined by the time t passed since the last pumping, i.e. $\hat{\rho}(t + m\tau) = \hat{\rho}(t)$, with $m = 0, 1, 2..$. The density operator is then given by

$$\hat{\rho}(t) = \mathrm{e}^{\mathcal{L}t}\mathcal{R}\mathrm{e}^{\mathcal{L}(\tau - t)}\hat{\rho}(t), \quad 0 < t < \tau, \quad (4)$$

where $\mathcal{R}\hat{\gamma} = \hat{R}\hat{\gamma}\hat{R}^\dagger$.

The probe consists of a non-invasive charge detector (not shown in Fig. 1), monitoring the individual dot-lead tunneling events in time [34, 35]. Since tunneling into (out of) the DQD creates a hole (an electron) excitation in the lead, we here consider the statistics of electron and hole transfers into the lead per pumping cycle. The full counting statistics for a time periodic system can be obtained along the lines of [41]. We introduce an electron (hole) counting field χ_e (χ_h) into the Liouvillian of Eq. (3), so that $\mathcal{L} \rightarrow \mathcal{L}(\chi_e, \chi_h)$. The cumulant generating function (CGF) over $N \geq 1$ periods is

$$\mathcal{S}_N(\chi_e, \chi_h) = \ln[\langle[\mathcal{R}\mathrm{e}^{\mathcal{L}(\chi_e, \chi_h)\tau}]^N\rangle_0], \quad (5)$$

where $\langle\hat{\gamma}\rangle_0 = \mathrm{tr}[\hat{\gamma}\hat{\rho}(0)]$. From the CGF one obtains the mean and variance of the number of electrons (holes) emitted per period as

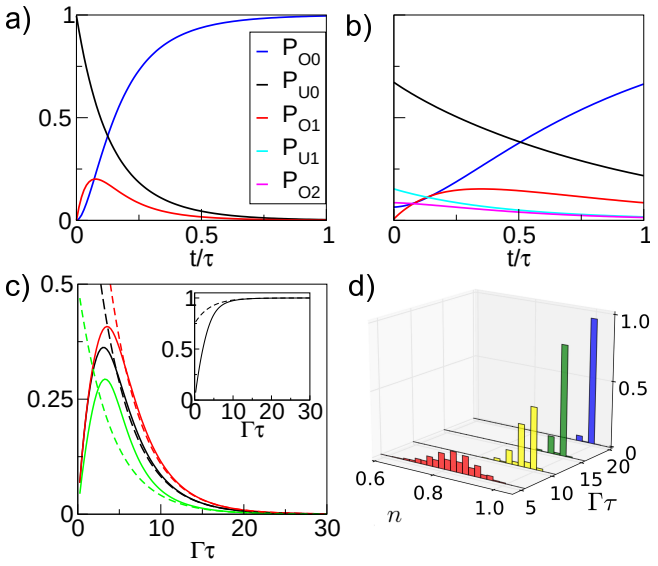

FIG. 3: (color online) a), b) Time-dependent probabilities of the TC-eigenstates (see text) for complete, a), and incomplete, b), transfer cycles. Legend in b) same as in a). c) Electron (green lines) and hole (red lines) noise as a function of $\Gamma\tau$, for $N = 1$. For $N \gg 1$ (black lines) electron and hole noise coincide. Inset: Average number of excitations $\langle n\rangle$ as a function of $\Gamma\tau$. In both main panel and inset, the numerical (solid lines) and analytical, large $\Gamma\tau$ (dashed lines) results, are shown. d) Full probability distribution $P_N(n)$ (for $N = 50$) for different $\Gamma\tau$.

$\langle n_{e(h)}\rangle_N = (1/N)\partial S_N/\partial(i\chi_{e(h)})|_{\chi_e,\chi_h=0}$ and $\langle \delta n^2_{e(h)}\rangle_N = (1/N)\partial^2 S_N/\partial(i\chi_{e(h)})^2|_{\chi_e,\chi_h=0}$. Moreover, the probability of emitting n_e electrons and n_h holes per period, during N periods, is given by $P_N(n_e,n_h) = \int_{-\pi}^{\pi} d\chi_e d\chi_h e^{-iN(n_e\chi_e+n_h\chi_h)+S_N(\chi_e,\chi_h)}/(2\pi)^2$.

Strong coupling regime.– To illustrate in a compelling way the proposed pump-probe scheme, we consider the strong coupling regime $g_0 \gg \Gamma$ and a period $\tau \gg 1/g_0$ (Fig. 3). In this regime vacuum Rabi oscillations are fast and can be averaged out in the density matrix (secular approximation). The QME then reduces to an ordinary master equation in the TC-basis, with the dynamics determined by Γ and τ. For long periods $\tau \gg 1/\Gamma$ the system will describe a complete cycle of transferring one energy quantum from the qubit, via a cavity photon, to an electron-hole pair excitation in the lead (see Fig. 2a). This picture is substantiated by the electron-photon dynamics, illustrated by the corresponding time dependent probabilities $P_{\sigma q}$ for the (set of) TC-eigenstates, shown in fig. 2b. Here σ denotes an empty (U) or occupied (O) dot and q the number of excitations. We stress that in this long period regime the system acts as an ideal electron-hole pair pump, or equivalently, a pump of energy quanta $\hbar\omega$.

Decreasing the period τ there are corrections to the complete transfer cycle. This is clear from the plot of the TC probabilities in Fig. 2b: higher energy states with $q = 2$, including two cavity photons, acquire a finite population. Importantly, the effect of finite $\Gamma\tau$ is clearly manifested in the full counting statistics. A careful inspection of Eq. (4) shows that the corrections scale as $x = e^{-\Gamma\tau/4}$, much smaller than unity for large $\Gamma\tau$. Solving the CGF to leading order in x we get

$$\frac{S_N(\chi_e,\chi_h)}{N} = i(\chi_e+\chi_h) + \frac{x(e^{-2i(\chi_e+\chi_h)}-1)}{8} + \frac{x\delta S}{N}. \quad (6)$$

The first term describes the complete cycle, while the second term describes the first order corrections. The third term $\delta S = (\cos(\chi_h)-4)/3 + [5e^{-i(\chi_e+\chi_h)} + 3e^{i(\chi_e+\chi_h)} - (e^{-2i(\chi_e+\chi_h)}-1)]/8$ gives the short time behavior, going to zero for $N \gg 1$. Focusing on the $N \gg 1$ limit, the electron and hole transfer statistics become identical, with the number of transferred excitations $n = n_e = n_h$, and we can write the full distribution (first order in x)

$$P_N(n) = (1-x/8)\delta_{n1} + (x/8)\delta_{Nn,N-2}. \quad (7)$$

From Eq. (7) as well as from the plot of the numerically evaluated $P_N(n)$, in Fig 3, it is clear that the effect of x is i) a non-zero probability for $N-2$ excitations to be transferred, and consequently, ii) a reduced probability for the ideal cycle, transferring N excitations. This can be explained as follows: for non-zero x there is a finite probability that an excitation is pumped out of the system during a qubit ramp. The $P_N(n)$ to leading order in x describes one such event during N cycles. When an excitation is pumped out of the system it does not generate an electron-hole pair. Moreover, during the subsequent period the system will remain in the ground state, where no electron-hole emission can occur, thus resulting in a total loss of two periods for missed excitations. We note that a similar mechanism was discussed in [42].

For arbitrary $\Gamma\tau$, the numerically calculated probability distribution $P_N(n)$ (for $N \gg 1$) as well as the two lowest cumulants for the electron and hole transfer statistics are shown in Fig. 3. The $P(n)$ shows that the "missed two excitations" effect, for $\Gamma\tau \sim 1$, turns into a "missed several pairs of excitations" effect, with a finite probability for missing an even number of excitations $2, 4, 6, ...$ The probability to miss an odd number of excitations is smaller, albeit increasing for decreasing $\Gamma\tau$.

The average number of emitted electrons and holes are equal and independent of N, $\langle n_e\rangle_N = \langle n_h\rangle_N = \langle n\rangle$. In Fig. 3 $\langle n\rangle$ is plotted together with the analytical solution for large $\Gamma\tau$, $\langle n\rangle = 1 - e^{-\Gamma\tau/4}/4$, following from Eq. (6). For $\Gamma\tau \gtrsim 10$ the two results coincide, while for smaller $\Gamma\tau$ the analytical solution overestimates the number of emitted excitations.

In contrast to the average number, the electron and hole noise differ for $N \sim 1$ while for $N \gg 1$ we find $\langle \delta n^2_e\rangle_N = \langle \delta n^2_h\rangle_N \equiv \langle \delta n^2\rangle$. As shown in Fig. 3, for $\Gamma\tau \gg 1$, both the electron and hole noise, for any N, are well captured by the large $\Gamma\tau$ approximation, $\langle \delta n^2_e\rangle_N =$

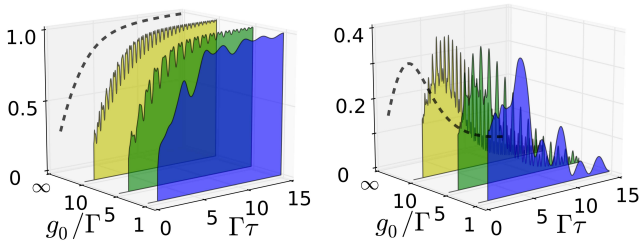

FIG. 4: (color online) Manifestation of vacuum Rabi oscillations. The average $\langle n\rangle$ (left panel) and fluctuations $\langle \delta n^2\rangle$ (right panel) of number of transferred electron hole pairs per pumping period as a function of $\Gamma\tau$ for different g_0/Γ. Dashed line (in both panels) is strong coupling result ($g_0 \gg \Gamma$).

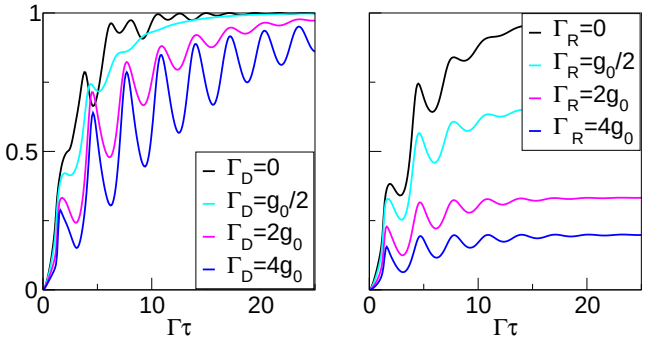

FIG. 5: (color online) Effects of dephasing and relaxation. Average number of excitations $\langle n\rangle$ as a function of $\Gamma\tau$ for different dephasing rates Γ_D, with $\Gamma_R = 0$ (left panel) and different relaxation rates Γ_R, with $\Gamma_D = g_0$ (right panel).

$[(N+1)/2N]\mathrm{e}^{-\Gamma\tau/4}$ and $\langle \delta n_h^2\rangle_N = [(3N+5)/6N]\mathrm{e}^{-\Gamma\tau/4}$, obtained from Eq. (6). The noise is thus exponentially suppressed when the number of excitations per period (exponentially) approaches unity. We point out that the difference between $\langle \delta n_e^2\rangle_N$ and $\langle \delta n_h^2\rangle_N$ for $N \sim 1$ is a consequence of electron and hole emission occurring at different times during the pumping period. Hence, this electron-hole asymmetry is altered if the measurement period is shifted with respect to the pumping period. During the rest of the paper we consider the $N \gg 1$ limit, when this asymmetry can be neglected.

Vacuum Rabi oscillations – Outside the strong coupling regime, i.e. for $\Gamma \sim g_0$, the coherent electron-photon dynamics becomes accessible. Focusing on period times τ comparable to $1/\Gamma, 1/g_0$ signatures of vacuum Rabi oscillations appear in the charge transfer statistics. This is clearly illustrated in Fig. 4, showing the average, $\langle n\rangle$, and fluctuations, $\langle \delta n^2\rangle$ of the number of transferred electron-hole pairs per period, as a function of $\Gamma\tau$. For both $\langle n\rangle$ and $\langle \delta n^2\rangle$, moving out of the regime $g_0 \gg \Gamma$ the vacuum Rabi oscillations are manifested as oscillations superimposed on the strong coupling result.

The connection between the vacuum Rabi oscillations and the superimposed oscillations in Fig. 4 can be illustrated by considering two opposite cases of pumping periods: When $\tau \approx 2\pi n/[\sqrt{2}g_0]$ ($\tau \approx 2\pi(n+1/2)/[\sqrt{2}g_0]$) the pumping occurs when the qubit has an increased probability to be excited (in the ground state). As a consequence, the pumping will with enhanced probability remove (add) an excitation, thereby decreasing (increasing) the number of electron-hole pairs created.

DQD relaxation and dephasing – In recent conductor-cavity experiments [4–9] DQD decoherence prevented reaching the strong coupling regime. This raises the question how the signatures of coherent electron-photon interaction in transport quantities are altered in the presence of dephasing and relaxation. Dephasing and relaxation, with rates Γ_D and Γ_R respectively, are accounted for by adding the terms $\mathcal{L}_D[\hat\rho] = \frac{\Gamma_D}{2}\mathcal{D}[\hat d_e^\dagger \hat d_e - \hat d_g^\dagger \hat d_g, \hat\rho]$ and $\mathcal{L}_R[\hat\rho] = \frac{\Gamma_R}{2}\mathcal{D}[\hat d_e^\dagger \hat d_g, \hat\rho]$ to the Liouvillian in Eq. (4).

The effect of dephasing is to suppress the coherence between the excited, $|e\rangle$, and ground, $|g\rangle$, states of the DQD. As illustrated in Fig. 5 this has several consequences for the average number of transferred excitations $\langle n\rangle$ (similarly for the fluctuations, not shown). Increasing the dephasing from $\Gamma_D \ll g_0$ the amplitude of the vacuum Rabi oscillations are first suppressed, reaching a minimum around $\Gamma_D \sim g_0$. However, increasing the dephasing further the oscillations are revived for $\Gamma_D > g_0$. In this strongly dephased regime the system can be seen as a coherent qubit-cavity subsystem, displaying vacuum Rabi oscillations with frequency $2\sqrt{2}g_0$, coupled incoherently to the DQD. Moreover, with increasing Γ_D the typical excitation escape time increases, i.e. the time it takes $\langle n\rangle$ to reach unity gets longer.

To investigate the effect of relaxation we fix $\Gamma_D = g_0$ and consider the dependence of $\langle n\rangle$ on Γ_R. The results are presented in Fig. 5. We see that the complete cycle is no longer reached, i.e. $\langle n\rangle < 1$ for $\Gamma\tau \gg 1$. This can be explained by the fact that relaxation in the DQD provides the system with a new mechanism of energy relaxation that is independent of any pumping events. From this discussion it is clear that dephasing and relaxation show up as distinct features in transport properties when the period time τ is tuned.

Conclusions and estimates.– In conclusion we have proposed and analyzed a pump-probe scheme for transient electron-photon dynamics in a hybrid DQD-cavity-qubit systems. We showed that key features of the dynamics can be investigated via the short time charge transfer statistics at the DQD. The dynamics was investigated in the presence of DQD dephasing and relaxation, considering the experimentally relevant situation with rates $g_0 \sim \Gamma_D, \Gamma_R \sim 100$MHz. Note that accessing the full transfer statistics on the time scale $1/g_0$ would require an improved charge counting rate, presently below 1MHz, and/or smaller DQD dephasing and relaxation. The first two moments, current and noise, could however be investigated by high-frequency measurements [43].

Acknowledgements– We acknowledge support from the

Swedish VR and the nanometer structure consortium at Lund university. We also thank Christian Flindt for providing constructive comments on the manuscript.

[1] T. Frey, P. J. Leek, M. Beck, K. Ensslin, A. Wallraff, and T. Ihn, Appl. Phys. Lett. **98**, 262105 (2011).

[2] M. R. Delbecq, V. Schmitt, F. D. Parmentier, N. Roch, J. J. Viennot, G. Fève, B. Huard, C. Mora, A. Cottet, and T. Kontos, Phys. Rev. Lett. **107**, 256804 (2011).

[3] M. R. Delbecq, L. E. Bruhat, J. J. Viennot, S. Datta, A. Cottet, and T. Kontos, Nature Comm. **4**, 1400 (2013).

[4] T. Frey, P. J. Leek, M. Beck, A. Blais, T. Ihn, K. Ensslin, and A. Wallraff, Phys. Rev. Lett. **108**, 046807 (2012).

[5] H. Toida, T. Nakajima, and S. Komiyama, Phys. Rev. Lett. **110**, 066802 (2013).

[6] K. D. Petersson, L. W. McFaul, M. D. Schroer, M. Jung, J. M. Taylor, A. A. Houck, and J. R. Petta, Nature **490**, 380 (2012).

[7] J. J. Viennot, M. R. Delbecq, M. C. Dartiailh, A. Cottet, and T. Kontos, arXiv:1310.4363 (2013).

[8] G.-W. Deng, D. Wei, J. R. Johansson, M.-L. Zhang, S.-X. Li, H.-O. Li, G. Cao, M. Xiao, T. Tu, G.-C. Guo, et al., arXiv:1310.6118 (2013).

[9] Y.-Y. Liu, K. D. Petersson, J. Stehlik, J. M. Taylor, and J. R. Petta, arXiv:1401.7730 (2014).

[10] M. Trif, V. N. Golovach, and D. Loss, Phys. Rev. B **77**, 45434 (2008).

[11] A. Cottet and T. Kontos, Phys. Rev. Lett. **105**, 160502 (2010).

[12] P.-Q. Jin, M. Marthaler, A. Shnirman, and G. Schön, Phys. Rev. Lett. **108**, 190506 (2012).

[13] A. Cottet, C. Mora, and T. Kontos, Phys. Rev. B **83**, 121311 (2011).

[14] J. Basset, D.-D. Jarausch, A. Stockklauser, T. Frey, C. Reichl, W. Wegscheider, T. M. Ihn, K. Ensslin, and A. Wallraff, Phys. Rev. B **88**, 125312 (2013).

[15] M. Schiró and K. Le Hur, arXiv:1310.8070 (2013).

[16] N. Lambert and F. Nori, Phys. Rev. B **78**, 214302 (2008).

[17] C. Bergenfeldt and P. Samuelsson, Phys. Rev. B **87**, 195427 (2013).

[18] N. Lambert, C. Flindt, and F. Nori, Europhys. Lett. **103**, 17005 (2013).

[19] L. D. Contreras-Pulido, C. Emary, T. Brandes, and R. Aguado, New J. Phys. **15**, 095008 (2013).

[20] C. Xu and M. G. Vavilov, Phys. Rev. B **88**, 195307 (2013).

[21] L. Childress, A. S. Sørensen, and M. D. Lukin, Phys. Rev. A **69**, 42302 (2004).

[22] P.-Q. Jin, M. Marthaler, J. H. Cole, A. Shnirman, and G. Schön, Phys. Rev. B **84**, 035322 (2011).

[23] A. Cottet, T. Kontos, and A. L. Yeyati, Phys. Rev. Lett. **108**, 166803 (2012).

[24] C. Bergenfeldt and P. Samuelsson, Phys. Rev. B **85**, 045446 (2012).

[25] T. L. Schmidt, A. Nunnenkamp, and C. Bruder, Phys. Rev. Lett. **110**, 107006 (2013).

[26] A. Cottet, T. Kontos, and B. Douçot, Phys. Rev. B **88**, 195415 (2013).

[27] C. Müller, J. Bourassa, and A. Blais, Phys. Rev. B **88**, 235401 (2013).

[28] C. Xu and M. G. Vavilov, Phys. Rev. B **87**, 035429 (2013).

[29] C. Bergenfeldt, P. Samuelsson, B. Sothmann, C. Flindt, and M. Büttiker, Phys. Rev. Lett. in press. (2014).

[30] H. Wang, M. Hofheinz, M. Ansmann, R. C. Bialczak, E. Lucero, M. Neeley, M. D. O'Connell, D. Sank, M. Weides, J. Wenner, et al., Phys. Rev. Lett **103**, 200404 (2009).

[31] M. Hofheinz, E. M. Weig, M. Ansmann, R. C. Bialczak, E. Lucero, M. Neeley, A. D. Oconnell, H. Wang, J. M. Martinis, and A. N. Cleland, Nature **454**, 310 (2008).

[32] M. Hofheinz, H. Wang, M. Ansmann, R. C. Bialczak, E. Lucero, M. Neeley, A. D. O'Connell, D. Sank, J. Wenner, J. M. Martinis, et al., Nature **459**, 546 (2009).

[33] C. Eichler, D. Bozyigit, C. Lang, L. Steffen, J. Fink, and A. Wallraff, Phys. Rev. Lett. **106**, 220503 (2011).

[34] S. Gustavsson, R. Leturcq, B. Simovič, R. Schleser, T. Ihn, P. Studerus, K. Ensslin, D. Driscoll, and A. Gossard, Phys. Rev. Lett. **96**, 076605 (2006).

[35] C. Flindt, C. Fricke, F. Hohls, T. Novotnỳ, K. Netočnỳ, T. Brandes, and R. J. Haug, Proc. Natl. Acad. Sci. **106**, 10116 (2009).

[36] J. Koch, T. M. Yu, J. Gambetta, A. A. Houck, D. I. Schuster, J. Majer, A. Blais, M. H. Devoret, S. M. Girvin, and R. J. Schoelkopf, Phys. Rev. A **76**, 042319 (2007).

[37] A. Wallraff, D. I. Schuster, A. Blais, L. Frunzio, R. S. Huang, J. Majer, S. Kumar, S. M. Girvin, and R. J. Schoelkopf, Nature **431**, 162 (2004).

[38] J. A. Schreier, A. A. Houck, J. Koch, D. I. Schuster, B. R. Johnson, J. M. Chow, J. M. Gambetta, J. Majer, L. Frunzio, M. H. Devoret, et al., Phys. Rev. B **77**, 189502 (2008).

[39] H. Wang, M. Hofheinz, J. Wenner, M. Ansmann, M. Bialczak, R C Lenander, , E. Lucero, M. Neeley, M. D. O'Connell, D. Sank, et al., App. Phys. Lett **95**, 233508 (2009).

[40] M. D. Reed, L. DiCarlo, S. E. Nigg, L. Sun, L. Frunzio, S. M. Girvin, and R. J. Schoelkopf, Nature **482**, 382 (2012).

[41] F. Pistolesi, Phys. Rev. B **69**, 245409 (2004).

[42] M. Albert, C. Flindt, and M. Büttiker, Phys. Rev. B **82**, 041407 (2010).

[43] A. Mahe, F. D. Parmentier, E. Bocquillon, J. M. Berroir, D. C. Glattli, T. Kontos, B. Placais, G. Feve, A. Cavanna, and Y. Jin, Phys. Rev. B **82**, 201309 (2010).